XI International Conference on Computational Plasticity. Fundamentals and Applications
COMPLAS XI
E. Oñate, D.R.J. Owen, D. Peric and B. Suárez (Eds)

DETERMINATION OF THE HIGH STRAIN RATE FORMING PROPERTIES OF STEEL SHEET

P. VERLEYSEN[*], J. PEIRS[*] AND L. DUCHENE [†]

[*] Department of Materials Science and Engineering
Faculty of Engineering
Ghent University
Technologiepark 903, 9052 Zwijnaarde (Ghent), Belgium
e-mail: Patricia.Verleysen@UGent.be, www.ugent.be/ir/dmse/en

[†] Mécanique des Solides, des Fluides et des Structures
Department ArGEnCO
University of Liege
Sart Tilman B52, 4000 Liège 1, Belgium
e-mail: L.Duchene@ulg.ac.be

Key words: Forming Process, Steel Sheets, Forming Limit Diagram.

Abstract. The strain rate dependence of the plastic yield and failure properties displayed by most metals affects energies, forces and forming limits involved in high speed forming processes. In this contribution a technique is presented to assess the influence of the strain rate on the forming properties of steel sheets. In a first step, static and high strain rate tensile experiments are carried out in order to characterize the materials strain rate dependent behaviour. In a second step, the phenomenological Johnson-Cook model and physically-based Voce model are used to describe the constitutive material behaviour. The test results are subsequently used to calculate the forming limit diagrams by a technique based on the Marciniak-Kuczynski model. With the developed technique, static and dynamic forming limit diagrams are obtained for a commercial DC04 steel and a laboratory made CMnAl TRIP steel. The results clearly indicate that increasing the strain rate during a forming process can have a positive or negative effect.

1 INTRODUCTION

In forming processes such as magnetic pulseforming, hydroforming and explosive forming, high rates of deformation are obviously obtained. However, also in more conventional sheet forming techniques, such as deep drawing, roll forming and bending, locally strain rates are occurring deviating from the ones occurring in static material tests. As the strain rate increases most materials present significantly higher plastic flow stresses, however much lower deformation levels. Other materials combine an increase in flow stresses with an increase in elongation values (Van Slycken et al., 2006). Materials which experience no strain rate sensitivity at all are exceptional. In the study here a commercial and laboratory made steel are considered. The commercial DC04 (EN 10027-1) is an unalloyed deep-drawing steel. This steel grade is frequently used in the production of body components in the automotive

industry. The laboratory made CMnAl-TRIP steel is a multiphase steel in which, under certain conditions, the austenite phase transforms to martensite during plastic straining [1].

In a first step, static and dynamic tensile experiments are carried out using a classical tensile test device and a split Hopkinson tensile bar facility respectively. The stress-strain curves obtained for the two steels clearly show that their mechanical behaviour is strain rate dependent. With increasing strain rate, plastic stress levels increase, however, as opposed to the TRIP-steel, for the DC04 steel the deformation capacity decreases. Subsequently, to allow simulation of forming processes, Johnson-Cook and Voce material model parameters are determined [2]. Finally, the influence of the strain rate on the forming limits is assessed using the uni-axial tensile test results. Indeed, performing multi-axial experiments at high strain rates is not obvious. Prediction of the initiation of necking in the steel sheets subjected to multi-axial strain states is based on the Marciniak-Kuczynski model. The thus obtained forming limit diagrams show a non-negligible effect of the strain rate. For the DC04 material, the reduced ductility at higher strain rates is reflected into an unfavourable downward shift of the forming limit diagram. Certainly, the left-hand side is adversely affected. The behaviour of the TRIP steel is as opposed to that of DC04: the dynamic FLD is higher than the static one.

2 EXPERIMENTAL PROGRAM

2.1 EXPERIMENTAL SETUPS

Static and dynamic tensile experiments are carried out at room temperature (around 22˚C). test bench. The *static experiments* are carried out on a classical screw driven electromechanical Instron tensile machine according to the European standard specifications EN 10002-1:2001. A tensile specimen, with a gage length of 120mm, is used in the tests. The tensile tests are carried out with an initial strain rate of 5.6 $10^{-4}s^{-1}$, in the gage section of the specimen, which is increased to 5.6 $10^{-3}s^{-1}$ at 3.4% of deformation until rupture.
For the *dynamic experiments* the split Hopkinson tensile bar (SHTB) setup of the department of Materials Science and Engineering at the Ghent University in Belgium is used. A schematic representation of the setup is given in the Figure 1, a photograph in the Figure 2.

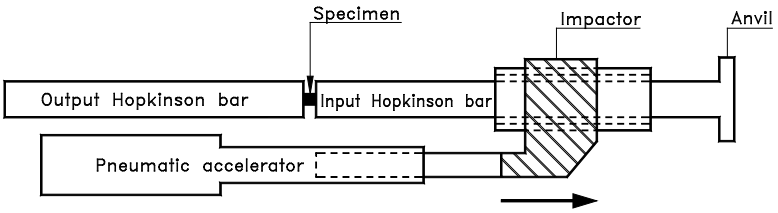

Figure 1: Schematic representation of split Hopkinson tensile bar device at Ghent University

The setup consists of two long bars, an input bar and an output bar, between which a specimen is sandwiched. For tensile tests a tube-like impactor is put around the input bar and is accelerated towards an anvil at the outer end of the input bar. Thus a tensile wave, the so-

called incident wave, is generated and propagates along the input bar towards the specimen. The incident wave interacts with the specimen, generating a reflected wave and a transmitted wave. The strain histories $\varepsilon_i(t)$, $\varepsilon_r(t)$ and $\varepsilon_t(t)$ corresponding to respectively the incident, reflected and transmitted wave are usually measured by means of strain gages at well chosen points on the Hopkinson bars. The history of the stress, the strain and the strain rate in the specimen are derived from the measured waves, using the following expressions [3]:

$$\sigma(t) = \frac{A_b E_b}{A_s} \varepsilon_t(t) \tag{1}$$

$$\varepsilon(t) = \frac{U_{ob} - U_{ib}}{L_s} = -\frac{2C_b}{L_s} \int_0^t \varepsilon_r(\tau) d\tau \tag{2}$$

$$\dot{\varepsilon}(t) = \frac{V_{ob} - V_{ib}}{L_s} = -\frac{2C_b}{L_s} \varepsilon_r(t) \tag{3}$$

with E_b the modulus of elasticity of the Hopkinson bars, A_s and A_b the cross section area of the specimen and of the Hopkinson bars respectively, C_b the velocity of propagation of longitudinal waves in the Hopkinson bars and L_s the gage length of the specimen. U_{ib} and U_{ob} are the displacements of the interface between the specimen and, respectively, the input bar and the output bar; V_{ib} and V_{ob} are the corresponding velocities.

Figure 2: SHTB setup at Ghent University. Its total length is 11m.

The DC04 sheet steel has a thickness of 1.5mm, the TRIP-steel 1.2mm. Specimens are cut by spark erosion along the rolling direction. Geometry and dimensions used for the split

Hopkinson tensile bar experiments can be found in Figure 3.

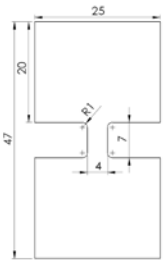

Figure 3: Geometry of test specimen used for the SHTB experiments. The 4mm wide section, with a gage length of 5mm, is actually submitted to the high strain rate load.

3.2 Results

Several static and dynamic tests have been carried out. In Figure 4 representative engineering stress-strain curves can be found. For the DC04 steel the static and dynamic curves have a different overall shape. For the static curve a clear strain hardening is observed during the first stages of plastic deformation and uniform elongation is achieved after 24% of deformation. The dynamic curves on the other hand, show a very high yield stress, again followed by few strain hardening. Between the dynamic curves differences are less pronounced.
The static and dynamic engineering stress-strain curves for the CMnAl TRIP steel are very similar. The stress increases, however not as much as for the DC04 steel. The main effect of the strain rate is seen in the higher uniform elongation during dynamic loading: ±30% vs ±22%.

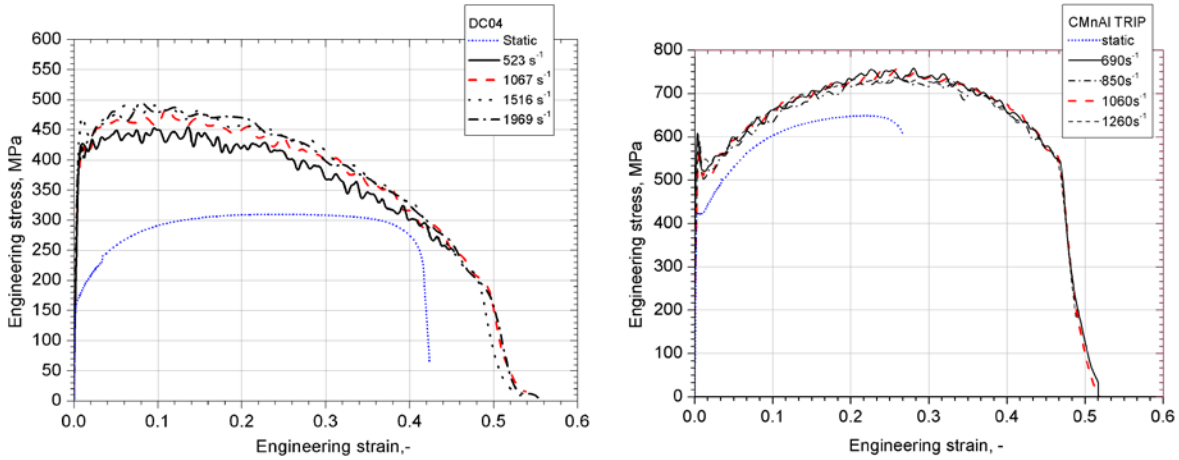

Figure 4: Representative static stress-strain curve and dynamic curves obtained for the investigated steels

3 MODELLING OF THE HIGH STRAIN RATE BEHAVIOUR

The experimental results are used to model the constitutive material behaviour. Two different frequently used models are used: Voce law and the Johnson-Cook model [2]. Voce law describes the relation between the stress σ and plastic strain ε_p. The model contains only three parameters σ_0, K and n which can easily be determined from only one experiment.

$$\sigma = \sigma_0 + K(1 - e^{-n\varepsilon_p}) \tag{4}$$

The Voce flow rule does not explicitly describe the material's strain rate and temperature dependence. Both can be taken into account by making the model parameters strain rate and/or temperature dependent.

The Johnson-Cook phenomenological model does take into account strain rate and temperature dependent material behaviour:

$$\sigma = \left(\mathrm{A} + \mathrm{B}\varepsilon_p{}^{\mathrm{n}}\right)\left(1 + C\ln\frac{\dot{\varepsilon}}{\dot{\varepsilon}_0}\right)\left(1 - \left[\frac{T - T_{room}}{T_{melt} - T_{room}}\right]^m\right) \tag{5}$$

The first term of the right hand side describes the isothermal static material behaviour. Consequently, the parameters A, B and n are determined using the static tensile tests. The initial (for ε<3.4%) strain rate during the static tensile test is the reference strain rate $\dot{\varepsilon}_0$ used in the second term, expressing the strain rate hardening with parameter C. The last factor, including m, represents thermal softening. C and m are calculated using the high strain rate tensile tests.

The quasi-adiabatic temperature increase in the specimen during high strain rate plastic deformation is calculated using the following formula:

$$\Delta T = \frac{\beta}{\rho c}\int \sigma d\,\varepsilon_p \tag{6}$$

In this equation ρ is the mass density, c the specific heat and β the Taylor-Quinney coefficient indicating the fraction of plastic work converted into heat. This β-value is usually assumed to have a value between 0.9 and 1. Constant values for c and β can be used regarding the modest temperature range acquired during these tests. During the high strain rate tests the temperature will gradually change from room temperature to approximately 100°C depending on the material.

In table 2 values for the parameters of Voce model σ_0, K and n and Johnson-Cook model A, B, n, C and m can be found. The parameters are calculated by a least square method. For the Voce law two sets of parameters are given: one for the static behaviour at room temperature and one for a dynamic, adiabatic experiment at $1000s^{-1}$.

In Figure 5 a comparison is made between experimental and modelled stress-strain curves. Both models succeed in describing the experimental behaviour. The Voce model appears to perform better than the Johnson-Cook model which is not surprising regarding the use of two Voce law parameter sets for the static and dynamic loading compared with one parameter set for the JC model. Indeed, the large differences between the overall shape of the static and dynamic stress strain curves complicates modelling of the material behaviour with one parameter set. Nevertheless, the agreement between the experiments and models is very good. Because the Voce model performs better at higher strains, it will be used for calculation of the FLDs in the next section.

Table 2: Values for the Voce and Johnson-Cook material model parameters

Model	Parameter	DC04	CMnAl TRIP
Voce (static/dynamic)	σ_0 (MPa)	163.5/383.1	394/501
	K	226.2/137.5	468/574
	n	13.2/31.7	9.2/5.4
Johnson-Cook	A (MPa)	162	394
	B (MPa)	598	1395
	n	0.6	0.72
	C	2.623	0.013
	m	0.009	0.62

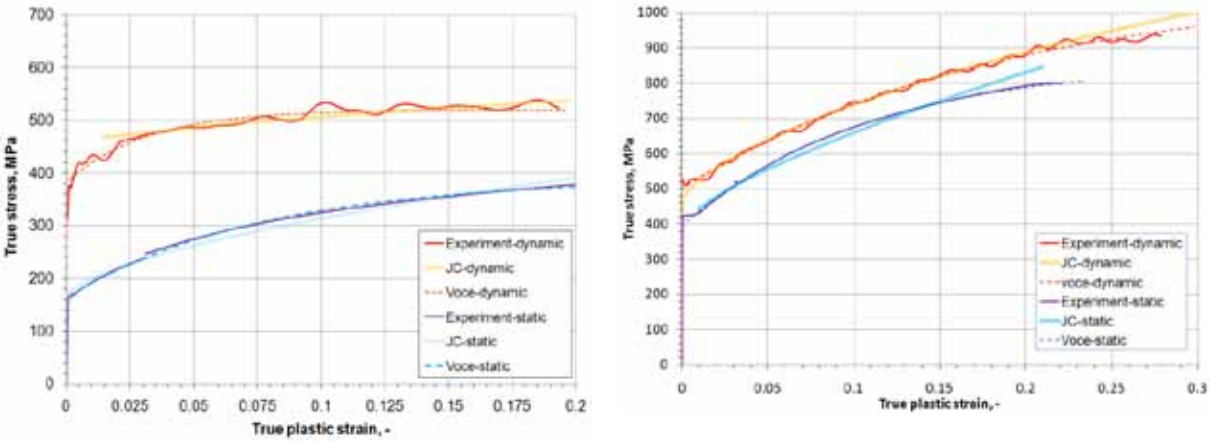

Figure 5: Experimental static and dynamic tensile curves and curves simulated with the Johnson-Cook model for the DC04 (left) and the TRIP (right) steel

4 CALCULATION OF STRAIN RATE DEPENDENT FLD

4.1 Marciniak-Kuczynski method

The uniaxial tensile test results at different strain rates are used to predict the forming limits of the studied steel grades. Onset of necking under the multi-axial strain conditions occurring in forming processes is predicted using the well-known Marciniak–Kuczinski model [5].

In the Marciniak-Kuczynski (MK) method, it is assumed that an initial imperfection is present in the sheet metal. The imperfection is modelled by a band b of smaller thickness than the surrounding zone a, as schematically represented in Figure 6. The orientation of the band is characterized by the angle ψ. The initial imperfection can originate from a real thickness variation, surface roughness, a local variation of the strength or a combination. Physical meaning of this assumption is given in [6]. The imperfection parameter, f_0, is defined as the ratio of the reduced thickness t_{b0} to the initial thickness of the sheet t_{a0} ($f_0=t_{b0}/t_{a0}$). During a biaxial straining process, the imperfection zone deforms more than the uniform zone. Therefore, the strain path of the imperfection zone is continuously ahead of the strain path of

the uniform zone. At a certain point, when the strain localization takes place, the difference between the strain path of the imperfection and the uniform zone begins to increase drastically. If the ratio of strain in the zone b to that of the perfect sheet reaches a presumed critical value, the sheet is considered to have failed. This critical value has low impact on the calculated forming limit because the strain in zone a does not change much once there is strain localization in b. The failure strain is calculated for different orientations of b. The lowest failure strain from these calculations is the forming limit. Once the strain localization is detected, the sheet metal is assumed to have failed.

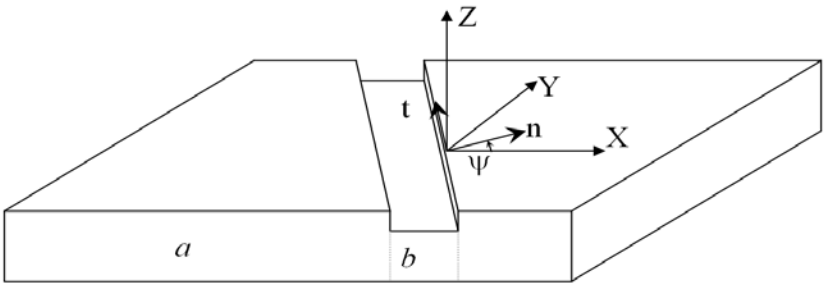

Figure 6: Schematic representation of the Marciniak-Kunczynski sheet with imperfection

In this study, the critical ratio of the strain increment in the region b to that of the region a is 4. The Voce hardening law fitted to the experimental stress-strain curves (see previous section) and von Mises yield criterion are adopted. Instead of optimizing the the imperfection parameter f_0, itis set on 0.99 for both materials for reasons of comparability.

4.2 Static and dynamic FLDs

The results of the FLD calculations are shown in Figure 7. Each chart presents a graph for static and a graph for dynamic ($1000s^{-1}$) deformation of the sheet.

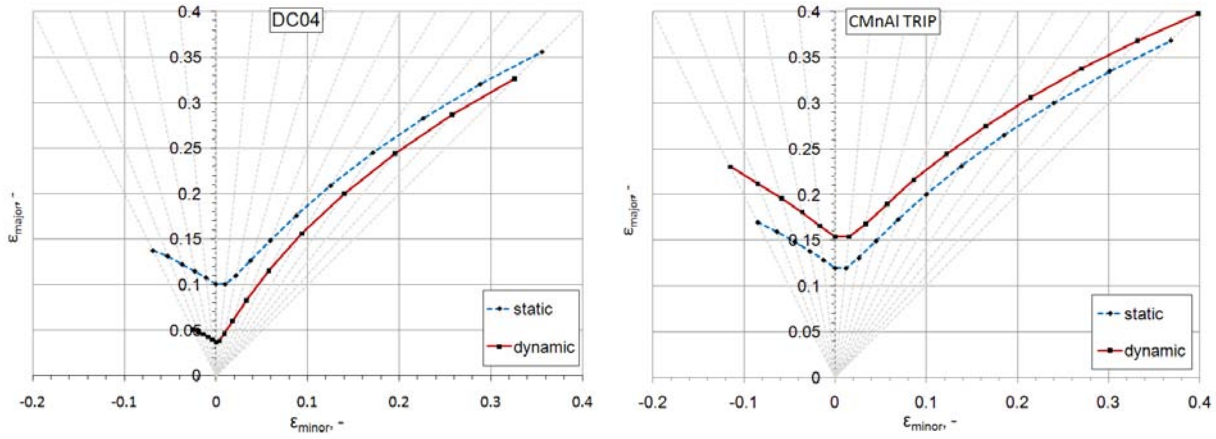

Figure 7: Comparison of static and dynamic FLD's for the considered steels

5 CONCLUSIONS

The influence of the strain rate on the forming properties of the commercial steels DC04 and a laboratory made CMnAl TRIP steel is studied. Static and high strain rate tensile experiments are performed to assess the influence of the strain rate on the mechanical behaviour. Going from static to dynamic loading rates, the plastic stresses increase. Concerning deformation before necking values are roughly halved for the DC04 steel. In contrast, the TRIP steel shows an increase of uniform strain when dynamically loaded. Subsequently, the Johnson-Cook and Voce models are used to describe the strain rate and temperature dependent constitutive behaviour of the studied steels. These constitutive models combined with the corresponding material parameters can be used to calculate the energies and forces occurring in a high speed forming process.

Finally, the influence of the strain rate on the forming limits is assessed using the uni-axial tensile test results. Prediction of the initiation of necking in the steel sheets subjected to multi-axial strain states is based on the Marciniak-Kuczynski model. The resulting forming limit diagrams show a non-negligible effect of the strain rate. The reduced ductility at higher strain rates is reflected into an unfavourable downward shift of the forming limit diagrams for the DC04 steel grade. For the TRIP steel, an important upward trend in the forming limits can be observed if the strain rate is increased.

REFERENCES

[1] Van Slycken, J., Verleysen, P., Degrieck, J., et al. High-strain-rate behavior of low-alloy multiphase aluminum- and silicon-based transformation-induced plasticity steels. *Met. Mat. Trans. A-Phys. Met. Mat. Sc.* (2006) **37A**:1527-1539.

[2] Liang, R.Q. and Khan, A.S. A critical review of experimental results and constitutive models for BCC and FCC metals over a wide range of strain rates and temperatures. *Int. J. Plast.* (1999) **15**:963-980.

[3] Kolsky, H. An investigation of the mechanical properties of materials at very high rates of loading Proc Phys Soc Lond Sec B (1949) **62**:676-700.

[4] Marciniak, Z. and Kuczynski, K. Limit strains in the processes of stretch-forming sheet metal, *Int. J. Mech.* (1967) **9**:609-620.

[5] Marciniak, Z., Kuczynski, K., and Pokora, T. Influence of plastic properties of a material on forming limit diagram for sheet-metal in tension. *Int. J. Mech. Sci.* (1973) **15**:789-800.